Redox Biology 21 (2019) 101069

Contents lists available at ScienceDirect

Redox Biology

journal homepage: www.elsevier.com/locate/redox

Research Paper

Endogenous cholesterol ester hydroperoxides modulate cholesterol levels and inhibit cholesterol uptake in hepatocytes and macrophages

Shuyuan Guo[a,b,c], Jianhong Lu[a,b], Yujuan Zhuo[a,b,c], Mengqing Xiao[a,b,c], Xinli Xue[a,b], Shanshan Zhong[a,b], Xia Shen[a,b,c], Chunzhao Yin[a,b,c], Luxiao Li[a,b,c], Qun Chen[a,b], Mingjiang Zhu[a], Buxing Chen[d], Mingming Zhao[e], Lemin Zheng[e], Yongzhen Tao[a], Huiyong Yin[a,b,c,f,*]

[a] CAS Key Laboratory of Nutrition, Metabolism and Food Safety, Shanghai Institute of Nutrition and Health, Shanghai Institutes for Biological Sciences (SIBS), Chinese Academy of Sciences (CAS), Shanghai 200031, China
[b] University of Chinese Academy of Sciences, CAS, Beijing 100049, China
[c] School of Life Science and Technology, ShanghaiTech University, Shanghai 200031, China
[d] Department of Cardiology, Beijing Tiantan Hospital, Capital Medical University, Beijing, China
[e] The Institute of Cardiovascular Sciences and Institute of Systems Biomedicine, School of Basic Medical Sciences, Key Laboratory of Molecular Cardiovascular Sciences of Ministry of Education, Peking University Health Science Center, Beijing, China
[f] Key Laboratory of Food Safety Risk Assessment, Ministry of Health, Beijing 100000, China

ARTICLE INFO

Keywords:
Cholesterol/metabolism
LDL oxidation
Lipidomics
CVD
Cholesterol ester hydroperoxides
Cholesterol uptake
Lipid peroxidation
LXR
LDLR

ABSTRACT

Dysregulation of cholesterol metabolism represents one of the major risk factors for atherosclerotic cardiovascular disease (CVD). Oxidized cholesterol esters (oxCE) in low-density lipoprotein (LDL) have been implicated in CVD but the underlying mechanisms remain poorly defined. We use a targeted lipidomic approach to demonstrate that levels of oxCEs in human plasma are associated with different types of CVD and significantly elevated in patients with myocardial infarction. We synthesized a major endogenous cholesterol ester hydroperoxide (CEOOH), cholesteryl-13(cis, trans)-hydroperoxy-octadecadienoate (ch-13(*c,t*)-HpODE) and show that this endogenous compound significantly increases plasma cholesterol level in mice while decrease cholesterol levels in mouse liver and peritoneal macrophages, which is primarily due to the inhibition of cholesterol uptake in macrophages and liver. Further studies indicate that inhibition of cholesterol uptake by ch-13(*c,t*)-HpODE in macrophages is dependent on LXRα-IDOL-LDLR pathway, whereas inhibition on cholesterol levels in hepatocytes is dependent on LXRα and LDLR. Consistently, these effects on cholesterol levels by ch-13(*c,t*)-HpODE are diminished in LDLR or LXRα knockout mice. Together, our study provides evidence that elevated plasma cholesterol levels by CEOOHs are primarily due to the inhibition of cholesterol uptake in the liver and macrophages, which may play an important role in the pathogenesis of CVD.

Non-standard abbreviations and acronyms: AA-CE, cholesteryl arachidonate; AMVN, 2, 2′-azobis(2,4-dimethylvaleronitrile); BEP-CE, Bicyclic endoperoxide and hydroperoxide cholesterol ester; BHT, butylated hydroxytoluene; BMDM, bone marrow-derived macrophage; BSTFA + TMCS, Bis-(trimethylsilyl)-trifluoroacetamide + Trimethylchlorosilane; CBD, cerebrovascular diseases; CE, cholesterol ester; CE19:0, cholesteryl nonadecanoate; CEOH, CE hydroxide; CEOOH, cholesterol ester hydroperoxide; CHD, coronary heart disease; CVD, cardiovascular disease; ch-13*c,t*-HpODE, cholesteryl-13(cis, trans)-hydroperoxy-octadecadienoate; ch-HpODE, cholesteryl-hydroperoxy-octadecadienoate; ch-HODE, cholesteryl-hydroxy-octadecadienoate; ch-HpETE, cholesteryl-hydroperoxy-eicosatetraenoate; ch-HETE, cholesteryl-hydroxy-eicosatetraenoate; chol-d7, cholesterol-d7; Dil-LDL, 1,1′-dioctadecyl-3,3,3′,3′-tetramethyl-indocarbocyanine perchlorate labeled LDL; GW, GW 3965; HMGCR, HMG-CoA reductase; IS, internal standard; IPA, isopropanol; IP, intraperitoneal injection; Idol, inducible degrader of the LDL receptor; LA-CE, cholesteryl linoleate; LA-CEOH, LA-CE hydroxide; LDL, low density lipoprotein; LXRα, liver X receptor α; LDLR, LDL receptor; MI, myocardial infarction; MRM, multiple reaction monitoring; mmLDL, minimally modified LDL; NH_4OAc, ammonium acetate; NaOMe, sodium methoxide; oxLDL, oxidized LDL; oxCE, oxidized CE; oxLA-CE, oxidized LA-CE; PPh_3, triphenylphosphine; PUFA, polyunsaturated fatty acid; RT, retention time; ROS, reactive oxygen species; SYK, spleen tyrosine kinase; TLR4, Toll like receptor 4; TLC, thin layer chromatography; T09, T0901317; WT, wide type

* Correspondence to: Shanghai Institutes for Biological Sciences, Chinese Academy of Sciences, Room 1826, New Life Science Bldg., 320 Yueyang Rd., Shanghai 200031, China.
E-mail address: hyyin@sibs.ac.cn (H. Yin).

https://doi.org/10.1016/j.redox.2018.101069
Received 15 November 2018; Accepted 6 December 2018
Available online 12 December 2018

1. Introduction

Cardiovascular disease (CVD) represents the leading cause of morbidity and mortality in the world. Furthermore, atherosclerosis and its clinical manifestations including ischemic heart diseases (myocardial infarction, MI) and cerebrovascular diseases (CBD), account for nearly 80% of the deaths of CVD [1]. Generally, elevated cholesterol level in the blood circulation is one of the major risk factors for atherosclerosis [2]. In addition to the cholesterol levels, cholesterol metabolites, such as oxysterols, play an important role in atherosclerosis [3,4]. As the major carriers of cholesterol to the peripheral tissues, low-density lipoprotein (LDL) particles are readily oxidized to form oxidized LDL (oxLDL) due to their abundant lipids containing polyunsaturated fatty acids (PUFA) in phospholipids and cholesterol esters [5,6]. A large body of evidence demonstrates that oxidized phospholipids on the surface of LDL are involved in atherosclerosis through multiple mechanisms, such as inducing inflammation and oxidative stress [7,8]. However, there are relatively limited studies regarding the roles of oxidized cholesterol esters (oxCE) on cholesterol metabolism in the context of atherosclerosis and the underlying molecular mechanisms remain poorly defined.

Cholesteryl linoleate (LA-CE) and cholesteryl arachidonate (AA-CE) are the major PUFA-containing CEs in the core of LDL. Under oxidative stress, these CEs readily undergo lipid peroxidation and generate hydroperoxides (CEOOH) as the major oxidation products in the complex oxidation mixture [9,10] and abundant oxCE have been detected in human atheroma and plasma [11–13]. However, the associations of CE oxidation products and CVD have not been well established. Furthermore, besides the effects on inflammation of oxCE [6], it remains to be investigated whether and how oxCE are involved in CVD through modulation of cholesterol metabolism including cholesterol uptake, transformation, efflux and excretion.

LDLR is the most important regulator for maintaining the levels of circulating LDL cholesterol (LDL-C) and reduced LDLR expression leads to the elevated cholesterol level in plasma [14]. Nuclear receptor liver X receptor (LXR) is an important factor regulating cholesterol homeostasis through LDLR and oxysterols are important endogenous activators of LXR [15]. Accumulating evidence suggests that LXR-IDOL (the inducible degrader of the LDLR)-LDLR axis plays an important role in regulating cholesterol level of plasma [16–18]. Even though activation of LXRα has been explored as an attractive strategy to treat atherosclerosis, synthetic agonists of LXR have only achieved limited success thus far due to the pleiotropic effects of LXR activation, such as the side effect of undesired hepatic steatosis [19]. Thus a better understanding of the molecular mechanisms by which cholesterol uptake is regulated may lead to a better therapeutic treatment of CVD [20]. It remains unexplored whether and how the LDLR and LXR is regulated by CEOOHs.

In this study, using a targeted lipidomic approach, we detected and quantified major oxCEs in the human plasma from different types of CVD and observed the changes of the levels of oxCEs in human plasma with CVD. Interestingly, the levels of oxLA-CE and oxAA-CE were significantly elevated in patient plasma of MI compared to control. Treatment of mice with ch-13(*c,t*)-HpODE, one of the major oxidation products of LA-CE, led to a significant elevation of plasma cholesterol while decreasing the cholesterol levels in liver and peritoneal macrophages. We further found that ch-13(*c,t*)-HpODE inhibited cholesterol uptake both in macrophage and hepatocytes. In macrophages, the inhibition of cholesterol uptake was mediated by the LXRα-IDOL-LDLR pathway, whereas in hepatocyte, the inhibition of cholesterol uptake was dependent on LXRα and LDLR. For the first time, our studies not only found an association of the levels of oxidized CEs in human plasma with CVD, but also uncovered a novel molecular mechanism by which cholesterol uptake in liver and macrophages is inhibited by endogenous CEOOHs.

2. Material and methods

2.1. Materials

LA-CE and cholesteryl nonadecanoate (CE19:0) were purchased from Nuchek Prep (Elysian, MN, USA). Cholesterol was purchased from Avanti Polar Lipids (Alabaster, AL, USA). Cholesterol-D7 (chol-d7) was purchased from Cambridge Isotope Laboratories, Inc (Andover, MA, USA). N-Methyl benzohydroxamic acid (NMBHA) was synthesized by our lab as described previously [21]. 2, 2′-azobis (2, 4-dimethylvaleronitrile) (AMVN) was purchased from J & K Scientific (Newark, DE, USA). Sodium methoxide (NaOMe), pyridine, triphenylphosphine (PPh_3), butylated hydroxytoluene (BHT), ammonium acetate (NH_4OAc), T0901317 (T09), 5α-cholestane, fatty acid free bovine serum albumin (BSA) were purchased from Sigma-Aldrich (Saint Louis, MO, USA). Bis-(trimethylsilyl)-trifluoroacetamide (BSTFA) + Trimethylchlorosilane (TMCS) was purchased from Supelco (Bellefonte, PA, USA). GW3965 (GW) was purchased from Selleck Chemicals (Houston, TX, USA). All solvents, such as hexane, isopropanol (IPA), were HPLC quality and purchased from Honeywell (Gibbstown, NJ, USA). 1,1′-dioctadecyl-3,3,3′,3′-tetramethyl-indocarbocyanine perchlorate labeled LDL (Dil-LDL) and LDL was purchased from Miao Tong Biological Technology (Shanghai, China). Thioglycollate medium (BD BBL™, Thioglycollate Medium Brewer Modified) was purchased from BD (Sparks, MD, USA).

2.2. Human samples

Human plasma samples were obtained from Beijing Tian Tan Hospital. The Institutional Review Board at Tian Tan Hospital approved the study and all participants provided with written informed consent. The human plasma from 49 human subjects were divided into four groups: healthy control group (con, n = 10), coronary heart disease group (CHD, n = 14), coronary heart disease and cerebrovascular disease group (CHD + CBD, n = 15), and myocardial infarction group (MI, n = 10). All participants in this study were diagnosed and classified based on symptoms and coronary angiography [7]. In brief, the control subjects were those the coronary angiography results did not show any lesions. The CHD group had at least one ≥ 50% stenotic lesion on coronary angiography. All subjects with CHD combined with an ischemic stroke were included in CHD + CBD, according to coronary angiography and cerebral angiography combined. And MI subjects had 100% stenotic lesion on coronary angiography. Coronary angiography was performed within 12 h of the onset of MI and the average time for blood collection was within 3–4 h. The blood samples were collected from overnight-fasted subjects and put into cold tubes containing EDTA (6 mmol/L). Plasma was prepared within 24 h by centrifugation (2500 g for 15 min) and aliquots immediately frozen at − 80 °C until analysis (avoid repeated freezing and thawing). The clinical information of human subjects was shown in Table 1.

The source and details of human postmortem samples were described previously [7]. The samples were immediately frozen (− 80 °C) after collection. The study was approved by the Institutional Review Board at Fudan University.

2.3. Animal experiments

All animal protocols were approved by the Institutional Animal Care and Use Committee of the Shanghai Institutes for Biological Sciences, Chinese Academy of Sciences. Male C57BL/6 mice (8–12 weeks old) were purchased from SLAC (Shanghai, China). The $LXR\alpha^{-/-}$ (C57BL/6) mice were gifts from Dr. Ben He's lab (Shanghai Jiao Tong University, Shanghai, China) [22]. Male $LDLR^{-/-}$ (C57BL/6) mice was purchased from Nanjing Biomedical Research Institute of Nanjing University (Nanjing, China). Mice were fed with chow diet, maintained in single-ventilated cages, and kept on a 12-h light/dark schedule. WT mice (8

Table 1
Clinical information of human subjects.

	CON	CHD	CBD + CHD	MI
Age (years)	56.2 ± 4.35	69 ± 2.37	69.13 ± 2.38	58.66 ± 5.58
Male gender (%)	70	69	60	90
BMI[a] (kg/m^2)	25.79 ± 0.65	24.47 ± 0.89	25.19 ± 0.73	26.67 ± 1.29
Smoking (%)	50	35.7	66.7	70
Drinking (%)	30	35.7	33.3	30
Hypertension (%)	100	85.7	93.3	30
Diabetes (%)	0	42.9	33.3	20
Statin (%)	80	64.2	100	40
Triglycerides (mg/dL)	1.76 ± 0.33	1.3 ± 0.17	1.36 ± 0.21	2.33 ± 0.62
TC[b] (mmol/L)	3.45 ± 0.19	3.77 ± 0.21	3.49 ± 0.16	4.65 ± 0.18**
LDL-C[c] (mmol/L)	1.86 ± 0.15	2.19 ± 0.18	1.90 ± 0.18	3.65 ± 0.76
HDL (mmol/L)	1.03 ± 0.06	0.99 ± 0.06	1.06 ± 0.07	1.03 ± 0.07
apo-A1 (g/L)	1.23 ± 0.09	1.2 ± 0.05	1.23 ± 0.06	1.32 ± 0.07
apo-B (g/L)	0.73 ± 0.04	0.81 ± 0.05	0.78 ± 0.04	1.08 ± 0.15

Values are the mean ± SEM. or percentage (%).
* $p < 0.05$, *versus* CON group.
[a] Body mass index.
[b] total cholesterol.
[c] LDL cholesterol.
** $p < 0.01$.

weeks old) were randomly divided into four groups: control group, ch-13(*c,t*)-HpODE group with different concentration (1 mg/kg, 1.5 mg/kg, 2.2 mg/kg). Control group: 0.745 mg/kg chol-d7 was dissolved in 0.9% saline containing 0.5% DMSO and 0.5% IPA.

Ch-13(*c,t*)-HpODE group: The ch-13(*c,t*)-HpODE with different concentration and 0.745 mg/kg (body weight) of chol-d7 were dissolved in 0.9% saline containing 0.5% DMSO and 0.5% IPA.

First, the mice were injected 1 ml thioglycollate medium for 4 days. Mice were treated for 24 h by an intraperitoneal (IP) injection of 200–250 μl 0.9% saline with the compounds (the injection volume adjusted to mouse body weight). Then the mice were anesthetized and sacrificed after fasting overnight. Liver, peritoneal macrophages and plasma were collected for cholesterol detection, real time quantitative polymerase chain reaction (RT-PCR), and Western blot. Similar experiments were performed for LXRα$^{-/-}$ and LDLR$^{-/-}$ mice.

2.4. Cell culture

Bone marrow cells collected from male C57BL/6 mice (8 weeks old) were cultured in RPMI medium supplemented with 20% fetal bovine serum (FBS) and 30% L929 supernatant to induce bone marrow derived macrophages (BMDMs).

Primary hepatocytes were isolated from the livers of male C57BL/6 mice (at least 12 weeks old) using collagenase perfusion as previously described [23]. Primary hepatocytes were cultured in DMEM supplemented with 10%FBS.

Peritoneal macrophages were isolated from mice by peritoneal lavage 4 days after IP injection of 1 ml thioglycollate medium (BD) according to a previous reference [24]. Before collecting the cells, the mice were treated with different compounds for 24 h. Then the cells were pooled together for detection without *in vitro* culture ($n \geq 5$).

Cell lines: HepG2, LM3, RAW264.7 were all cultured in DMEM containing 10% FBS. All cells were obtained from Cell Bank of Chinese Academy of Sciences (Shanghai, China).

For cell experiments, ch-13(*c,t*)-HpODE was dissolved in 0.05% DMSO and 0.05% IPA; control group only added 0.05% DMSO and 0.05% IPA. Then, cells were treated with control or ch-13(*c,t*)-HpODE in DMEM or RPMI medium containing 0.2% fatty acid free BSA. All cells were cultured in monolayer at 37 °C with 5% CO_2.

2.5. A Targeted lipidomic approach to analyze the oxCE in human plasma and atherosclerotic plaque

Plasma lipids were extracted using Folch solution (chloroform: methanol = 2:1, vol: vol, containing 0.005% BHT and 0.0025 mg/ml PPh3) as referenced [25,26]. In brief, 300 μl of plasma was added 700 μl 0.9% NaCl after CE (4 μg CE 19:0 in IPA) was added as IS. Then the samples were extracted with 4 ml ice-cold Folch solution twice. The combined organic phase was dried and the lipid extract was re-suspended in 100 μl hexane for analysis.

The procedure to extracted lipids followed our previously published protocol [7]. In brief, the human plaques were weighed and pulverized in liquid nitrogen before added 1 ml 0.9% NaCl. Then the extraction procedure was the same as the plasma.

2.5.1. Targeted lipidomics based on liquid chromatography and mass spectrometry (LC-MS)

The detection method was the same as in the reference with slight modification [27]. Normal phase LC was carried out with Agilent 1260 Quat pump VL and Accela 1250 pump. The column was Phenomenex 3-μm silica (2 mm × 250 mm). The samples were run at a flow rate of 200 μl/min in mobile (0.5% IPA in hexane). The eluent from normal-phase LC was mixed with 4 mM NH_4OAc in IPA at a flow rate of 200 μl/min prior to infusion into the MS. The MS was performed on a TSQ Vantage (Thermo Scientific). The MS was operated in positive ion and multiple reaction monitoring (MRM) mode. The transitions were listed in Table 2. Chromatographic peaks were integrated and area ratios (samples *versus* IS) were generated using Xcalibur (Thermo Scientific, San Jose, USA).

2.6. Formation, isolation and identification of ch-13(c,t)-HpODE

The procedures to prepare and characterize ch-13(*c,t*)-HpODE were reported previously [28,29]. A round-bottomed flask was added 0.2 M LA-CE (100 mg, 0.15 mmol), 0.2 M NMBHA (20 mg, 0.15 mmol) and 0.02 M AMVN (3.8 mg, 0.015 mmol) in dry acetonitrile. Then the flask was stirred at 37 °C under an oxygen atmosphere for 48 h. Normal phase HPLC was performed using a Waters 2690 HPLC instrument with a Waters 2998 PDA detector operating at 234 nm. The purity of the separated fractions was determined on an analytical column

Table 2
The MRM transitions of various oxCE in the targeted lipidomics.

Name		Parent mass (*m/z*)		Product mass(*m/z*)
		$(M+NH_4)^+$	$(M\text{-}NH_4)^+$	
1 LA-CEOOHs	a. ch-13(*c,t*)-HpODE b. ch-13(*t,t*)-HpODE c. ch-9-HpODE	698.6	680.6	369.3
2 LA-CEOHs	a. ch-13(*c,t*)-HODE b. ch-13(*t,t*)-HODE c. ch-9-HODE	682.6	664.6	369.3
3 AA-CEOHs	a. ch-15-HETE b. ch-12-HETE c. ch-11-HETE d. ch-9-HETE e. ch-8-HETE f. ch-5-HETE	706.6	688.6	369.3
4 AA-CEOOHs	a. ch-15-HpETE b. ch-12-HpETE c. ch-11-HpETE d. ch-9-HpETE e. ch-8-HpETE f. ch-5-HpETE	722.6	704.6	369.3

Phenomenex Luna-5-μm silica column (4.6 mm × 250 mm) (Torrance, CA, USA). A flow rate of 1.0 ml/min was used for analysis and 0.5% IPA in hexane was used as the solvent. Ch-13(*c,t*)-HpODE was reduced by PPh_3 and dried under nitrogen before adding 600 μl 1.86% NaOMe in methanol. After incubation at 50 °C for 10 min, the product was extracted three times by hexane. After evaporation, 40 μl of pyridine and 40 μl of BSTFA + TMCS were added into the tubes and were kept at 90 °C for an hour before subjected to GC-MS analysis. The instrument parameters were described in the GC-MS method of cholesterol uptake assay. The structures of the desired compounds were confirmed by the MS fragments: m/z = 225 and 311 for TMS-derivatized HODE methyl ester, and m/z = 329, 368, 458 for cholesterol.

2.7. Total cholesterol, ApoB, and ApoA1 assays

Total cholesterol, ApoB, and ApoA1 in plasma of mice were detected following the manufacturer's instructions (Total cholesterol/ApoB/ApoA1 detection reagent kit, China). The total cholesterol in liver and peritoneal macrophages were detected by GC-MS. For liver tissue, a liver sample (10–20 mg) was weighed and homogenized in 500 μl of ice-cold PBS buffer. For peritoneal macrophages, the cells were collecting from peritoneal cavity and pooled together without *in vitro* culture. The method of extraction and detection were generally the same as the cholesterol uptake assay. Specifically, the GC chromatograms was extracted at m/z = 329, 368, 458 for cholesterol and m/z = 217, 357 for IS. Calibration curves were generated using cholesterol standard and IS (5α-cholestane). The final results were normalized to protein concentration.

2.8. Cholesterol uptake assay

Radioactively labeled cholesterol has been commonly used for cholesterol uptake and recent studies also use stable isotope labeled cholesterol that can be readily detected by MS methods.

2.8.1. The extraction of total and free cholesterol-d7

Cells were treated with different compounds in the presence of 25 μg/ml LDL and 15 μg/ml chol-d7 for 24 h [30]. The extraction of cholesterol followed a protocol slightly modified from a previous reference [31]. After washing with PBS three times, the cells were collected and a 100μl aliquot of cell lysates was used to determine protein concentration by the BCA assay. Cellular cholesterol-d7 was extracted using 2 ml hexane: IPA (3:2, v/v) supplemented with 1% acetic acid and 5α-cholestane (6 μg) as internal standard (IS). The upper organic phase was collected after vortexing and centrifugation. Then the remaining aqueous phase was extracted one more time. The combined organic phase extract was equally divided into two parts. One part was dried under nitrogen for free cholesterol-d7 quantification after derivatization. For the detection of total cholesterol-d7, the other part was dried under nitrogen and added 200 μl 8 M KOH. After kept at 55 °C for 1 h, the mixture was added 8 M HCl to adjust to pH 3.0 before extraction with 2 ml IPA: hexane: acetic acid (40:10:1, v/v/v), 1 ml hexane and 1 ml water. Then the upper organic phase was separated after vortexing and centrifugation. The remaining aqueous phase was extracted one more time with 1 ml hexane. Then the combined organic phases were dried and added 40 μl of pyridine and 40 μl of derivatizing agent (BSTFA + TMCS). The mixtures were kept at 90 °C for an hour before the clear liquid was collected for GC-MS analysis. The standard (cholesterol-d7) with IS (5α-cholestane) was treated using the same methods. The total amount of cholesterol-d7 was used a reflection of cholesterol uptake.

2.8.2. Gas chromatography and mass spectrometry (GC-MS)

GC-MS was performed in the EI mode by using a Shimadzu GC-MS QP2010. The ion source temperature was set at 230 °C. The injection temperature was set at 250 °C. The cholesterol TMS derivatives were separated on an Rxi-5MS column (19 m, 0.25 mm inner diameter, 0.25 μm film thickness). The initial GC oven temperature was set at 110 °C , increased to 250 °C by 30 °C/min and held for 1 min, and then increased 10 °C/min to 280 °C for 1 min followed by 3 °C/min to 300 °C for 3 min. The GC chromatograms were extracted at m/z = 217 and 357 for IS, m/z = 336, 375, 465 for chol-d7. Their retention time (RT) were about 13.8 and 17.4 min, respectively. Then peak areas were integrated using the instrument software. Calibration curves were generated using chol-d7 and IS. The final results were normalized to protein content of cell lysates.

2.9. Dil-LDL uptake assay

Cells were treated with control (con) and 10 μg/ml ch-13(*c,t*)-HpODE for 24 h or 30 min. For Dil-LDL uptake assay, cells were incubated with 20 μg/ml Dil-LDL for 6 h or 8 h at 37 °C before washed with PBS. Then the cells were fixed with 1% paraformaldehyde and analyzed by flow cytometry (Guava® easyCyte 12, Millipore). The quantification of Dil-LDL uptake based on the intensities of fluorescence were recorded and normalized to control group.

2.10. Gene expression by RT-PCR

After treatment, cells and tissues were washed with PBS and lysed with TRIzol reagent (Invitrogen) and subjected to reverse transcription followed by RT-PCR (Takara) using Applied Biosystems 7900 instrument. The relative expressions of mRNAs were calculated using the comparative CT method and normalized to L32 or β-actin expression. Primer sequences are listed in Supplemental Table S1.

2.11. Western blot analysis

Cells were harvested by cell lysis for 30 min. For tissues, a liver sample (10–20 mg) was weighed and homogenized in 500 μl of tissue lysis. Proteins were separated by SDS-PAGE and transferred onto PVDF membranes. Immunoreactivity was developed with SuperSignal chemiluminescent substrate (Thermo Scientific). Primary antibodies used were anti-LDLR (1:1000, Proteintech, 10785–1-AP), anti-LXRα (1:1000, Proteintech, 14351–1-AP), anti-GAPDH (1:5000, Proteintech, 60004–1-Ig).

2.12. Statistical analysis

Results were shown as mean ± SEM. and analyzed by one or two-way ANOVA with appropriate *post-hoc* tests or an unpaired two tailed, Student's *t*-test. Statistical significance was set at $*p < 0.05$, $**p < 0.01$, $***p < 0.001$. Sample sizes, statistical tests for each experiment are depicted in the relevant figure legends. Data analysis was performed using GraphPad Prism Software 5.0.

3. Results

3.1. A targeted lipidomic analysis revealed the levels of oxCE in human plasma from various type of CVD

To investigate the levels of oxCE in human plasma associated with different types of CVD, we synthesized various standards of oxLA-CE and oxAA-CE and established a targeted lipidomic method based on normal phase LC coupled to MS to systematically quantify four major classes of oxCEs, including cholesteryl hydroperoxyl-octadecadienoate (ch-HpODE), cholesteryl-hydroxy-octadecadienoate (ch-HODE), cholesteryl hydroperoxy-eicosatetraenoate (ch-HpETE) and cholesteryl-hydroxy-eicosatetraenoate (ch-HETE). The chemical structures of these primary CE oxidation products have been characterized and synthetic standards were used for quantification purpose (Supplemental Fig. S1A-B) [10,28,32]. Then we detected these oxCE in plasma samples of 49

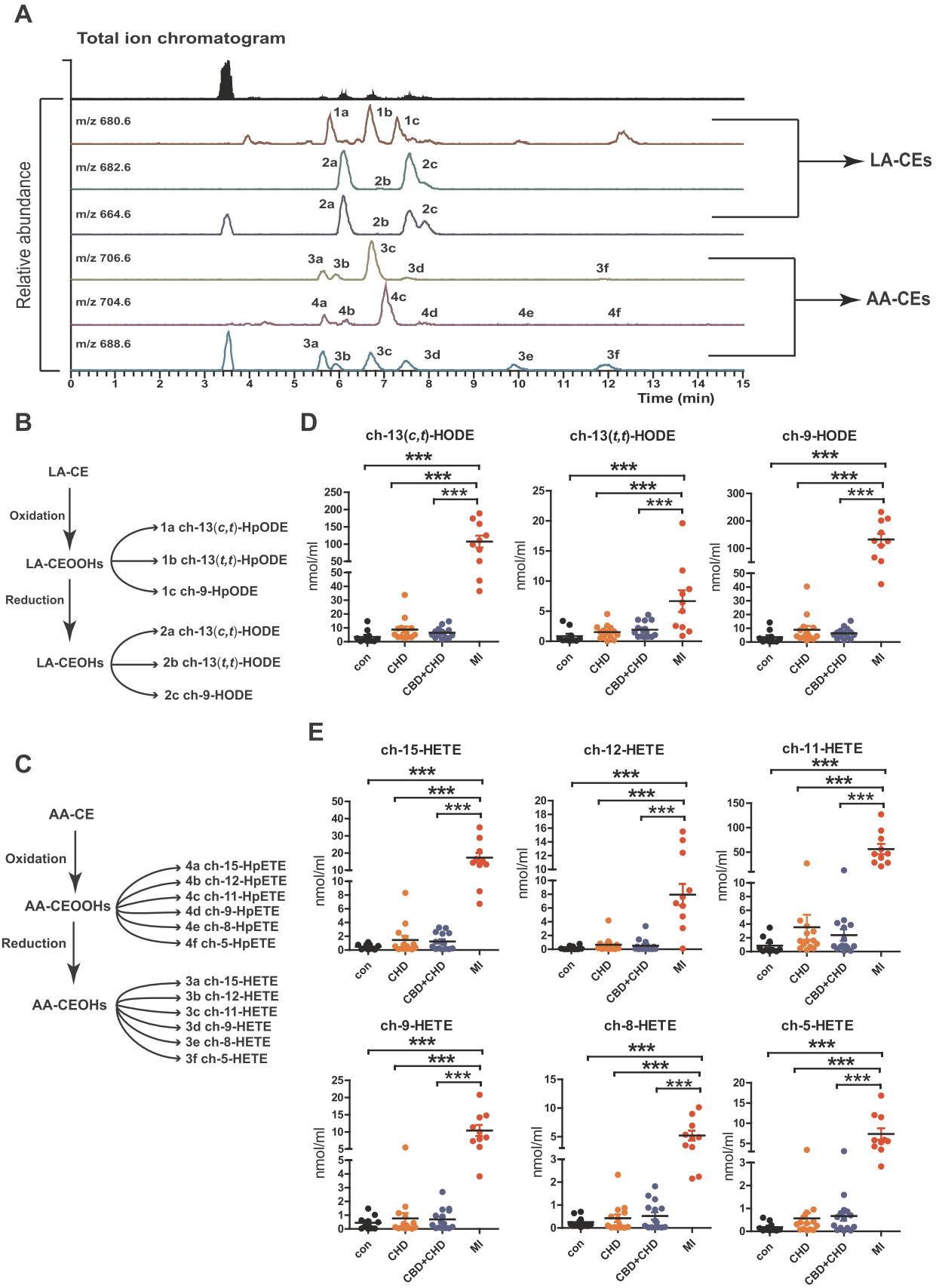

Fig. 1. The levels of oxCEs were significantly elevated in plasma of patients with MI. A. The MRM chromatogram of oxLA-CEs and oxAA-CEs in MI group detected by LC-MS/MS. The samples were not treated by PPh3 and other MS details were shown in Table 2. B-C. The transformation of oxidation products of LA-CEs and AA-CEs *in vivo* and *in vitro* (the labels of each product in chromatogram were shown in panel. A). D-E. Quantification results of major oxCE products in human plasma (Con: n = 10, CHD: n = 14, CBD + CHD: n = 15, MI: n = 10). Statistical analyses, one-way ANOVA with Bonferroni's test; *** $p < 0.001$.

CVD patients: control (con), coronary heart disease (CHD), CHD combined with cerebrovascular diseases (CHD + CBD), and MI group. The clinical information of these subjects was summarized in Table 1. Most of the baseline parameters were similar except that the total cholesterol and LDL-C are significantly higher in MI group compared to the other groups. We detected CEOOHs and CE hydroxides (CEOHs) in MI group and a representative chromatogram of these oxCEs were listed in Fig. 1A. The mass spectrometry parameters to quantify these oxCE were shown in Table 2. Interestingly, however, we only detected CEOHs in other three groups. Oxidation of LA-CEs and AA-CE initially formed CEOOHs including ch-HpODE and ch-HpETE, however, in the presence of reducing equivalents, such as glutathione (GSH) and GSH peroxidases [13], CEOOHs are readily reduced to CE hydroxides (CEOHs) both *in vivo* and *in vitro* (Fig. 1B-C). Thus it is not surprising that the levels of the corresponding CEOOHs are much lower than their reduced products in plasma.

To better quantify the levels of oxCE in human plasma and minimize *ex vivo* oxidation during sample preparation for LC-MS analysis, we converted all the CEOOHs to CEOHs with PPh_3 in the presence of antioxidant BHT. We quantified two major kinetic oxidation products of LA-CE, ch-13(*c,t*)-HODE and ch-9(*c,t*)-HODE, and one minor thermodynamic product, ch-13(*t,t*)-HODE (Fig. 1D) in the plasma and six major products of AA-CE: ch-5-HETE, ch-8-HETE, ch-9-HETE, ch-11-HETE, ch-12-HETE, and ch-15-HETE (Fig. 1E). Compared to control group, the levels of ch-HODE and ch-HETE were 2–3 folds higher in CBD and CBD + CHD group. Surprisingly, levels of ch-HODE were significantly associated with MI and the levels of ch-13(*c,t*)-HODE and ch-9-HODE reached around 100 μM in human plasma of MI patients (Fig. 1D). Furthermore, we found that the levels of ch-HETE were significantly higher in MI group compared to control, whereas these levels were relatively lower than ch-HODE (Fig. 1E). Based on the LC-MS results, we can see the obvious changes of LA-CEOHs (Supplemental Fig. S1C) and AA-CEOHs (Supplemental Fig. S1D) in MI compared to other groups.

As shown in Heatmap (Fig. 2A), the levels of oxCE were drastically elevated in MI group. Notably, the oxidation products of LA-CE, ch-13(*c,t*)-HODE and ch-9-(*c,t*)-HODE represented the largest components compared to other oxidation products in plasma samples of each group (Fig. 2B). As mentioned, our LC-MS quantified two different stereoisomers of ch-13-HODE, which included ch-13-(*c,t*)-HODE and ch-13-(*t,t*)-HODE, whereas the two isomers of ch-9-HODE did not readily separate. Generally, we observed more ch-13-HODE (sum of two isomers) than ch-9-HODE: 39% vs 29% in CON, 46% vs 32% in CHD, 45% vs 35% in CBD + CHD. However, MI group had 32% (ch-13-HODE) vs 38% (ch-9-HODE) (Fig. 2B). Next, we also analyzed the ratio of these oxidation products to total CE, un-oxidized LA-CE and un-oxidized AA-CE (Fig. 2C-E). We found that the ratios of LA-CEOHs were about 20% while AA-CEOHs was about 8% (Fig. 2C) in MI group. They together account for 25% of total CE, a similar extent of oxidation to those in the atherosclerotic plaques in previous reports [12]. And we also found the proportions of oxLA-CE/LA-CE and oxAA-CE/AA-CE were increased both in CHD and CBD + CHD group and significantly increased in MI group (Fig. 2D-E). In addition, we also detected similar patterns of CE oxidation products in human atherosclerotic plaques (Supplemental Fig. S1E). Different from those in the plasma, higher levels of the thermodynamic product ch-13(*t,t*)-HODE were observed in the plaques than those in the plasma (peak b in the Supplemental Fig. S1E), suggesting an exhaustion of antioxidants in the atherosclerotic plaque.

Collectively, all these data illustrate that a complex mixture of oxCE is readily detectable in human plasma from different types of CVD based on a targeted lipidomic approach. Furthermore, we found that the levels of oxCE in human plasma were positively associated with different types of CVD and significantly increased in MI subjects.

3.2. Treatment of mice with low doses of ch 13-(c,t)-HpODE regulated cholesterol levels in an LDLR and LXRα-dependent manner in vivo

According to the clinical data (Table 1), total cholesterol and LDL-C were higher in MI group whereas the HDL-C was not significantly changed, which prompted us to study the roles of these CE oxidation products on cholesterol metabolism. Ch-13(*c,t*)-HODE is one of the major oxidized products in human plasma and atherosclerotic plaque. As shown in Fig. 1B-C, oxidation of LA-CE and AA-CE initially generates cholesterol ester hydroperoxides (CEOOHs), which can be reduced to CEOHs by various reductants. Previous studies found that the biological activity of lipid hydroperoxide was diminished when they were reduced to CEOHs by Ebselen [33,34]. We hypothesize that CEOOHs are the major components in tissues eliciting biological activities in the context of CVD. Thus we set out to synthesize ch-13(*c,t*)-HpODE, one of the major the lipid hydroperoxide of LA-CE, and use it as a representative to study the roles of oxCE on cholesterol metabolism *in vitro* and *in vivo*.

The preparation, purification and characterization of ch-13(*c,t*)-HpODE were illustrated in Supplemental Fig. S2 according to our previous reports [21,28,29]. LA-CE was oxidized under free radical conditions to produce a mixture of LA-CEOOHs and we isolated the mixture of oxLA-CEs by HPLC. The chemical structure of the purified ch-13(*c,t*)-HpODE was consistent with previous literature as characterized by GC-MS method (Supplemental Fig. S2).

To study the stability and metabolic fate of ch-13(*c,t*)-HpODE in mice, we analyzed the levels of this compounds in mouse plasma after injected the mice with 1.5 mg/kg dose intraperitoneally. Interestingly, the basal levels of ch-13(*c,t*)-HpODE was below the detection limit (Supplemental Fig. S3A). However, the levels of ch-13(*c,t*)-HpODE reached 8.5 μM at 2 h and 5 μM at 24 h post injection (Supplemental Fig. S3A-B), respectively. The levels of ch-13(*c,t*)-HpODE are comparable to those in human plasma of CHD, CBD + CHD, and much lower than those from MI patients (Fig. 1D). Furthermore, this low dose of ch-13(*c,t*)-HpODE did not cause obvious hepatotoxicity as shown in the immunohistochemical staining of the liver tissue and the plasma levels of ALT (alanine aminotransferase) and AST (aspartate aminotransferase) (Supplemental Fig. S3C).

To study the effects of oxCE on cholesterol metabolism *in vivo*, we injected mice with different doses from 0, 1, 1.5–2.2 mg/kg and measured the cholesterol levels in plasma, liver tissue and peritoneal macrophages (Fig. 3A). Notably, the doses of 1, 1.5, 2.2 mg/kg of ch-13(*c,t*)-HpODE in our study corresponded to 1.4 nmol/g, 2.2 nmol/g, 3.2 nmol/g, respectively, which were much lower than those in the literature with mmLDL and oxLDL (10 μmol/g and 40 μmol/g) [35]. Interestingly, we observed dose-dependent increase of cholesterol and ApoB in plasma without affecting the levels of ApoA1 (Fig. 3B), whereas the total cholesterol levels of liver and peritoneal macrophages were significantly decreased (Fig. 3C-D).

LDLR is the most important receptor for maintaining cholesterol levels in the circulation, and it is widely expressed in liver and macrophages. Previous studies reported that activation of LXRα decreased cholesterol uptake through degradation of LDLR by IDOL [18]. To determine whether the changes of cholesterol levels both in plasma, liver and peritoneal macrophages are dependent on LDLR and LXRα, we performed similar experiments in $LXR\alpha^{-/-}$ and $LDLR^{-/-}$ mice treated with ch-13(*c,t*)-HpODE. As expected, the elevated cholesterol levels in mouse plasma induced by ch-13(*c,t*)-HpODE was completely abolished both in $LDLR^{-/-}$ and $LXR\alpha^{-/-}$ group (Fig. 3E). Consistently, the declining of the free and total cholesterol levels in liver caused by ch-13(*c,t*)-HpODE were also abolished in $LDLR^{-/-}$ and $LXR\alpha^{-/-}$ group (Fig. 3E). Similar results were obtained in peritoneal macrophages in which the decrease of cholesterol levels induced by ch-13(*c,t*)-HpODE was also abolished in $LDLR^{-/-}$ and $LXR\alpha^{-/-}$ group (Supplemental Fig. S3D).

Taken together, all these data demonstrate that CEOOHs are important modulators of cholesterol levels in plasma, liver and peritoneal macrophages; biologically comparable doses of CEOOHs cause a

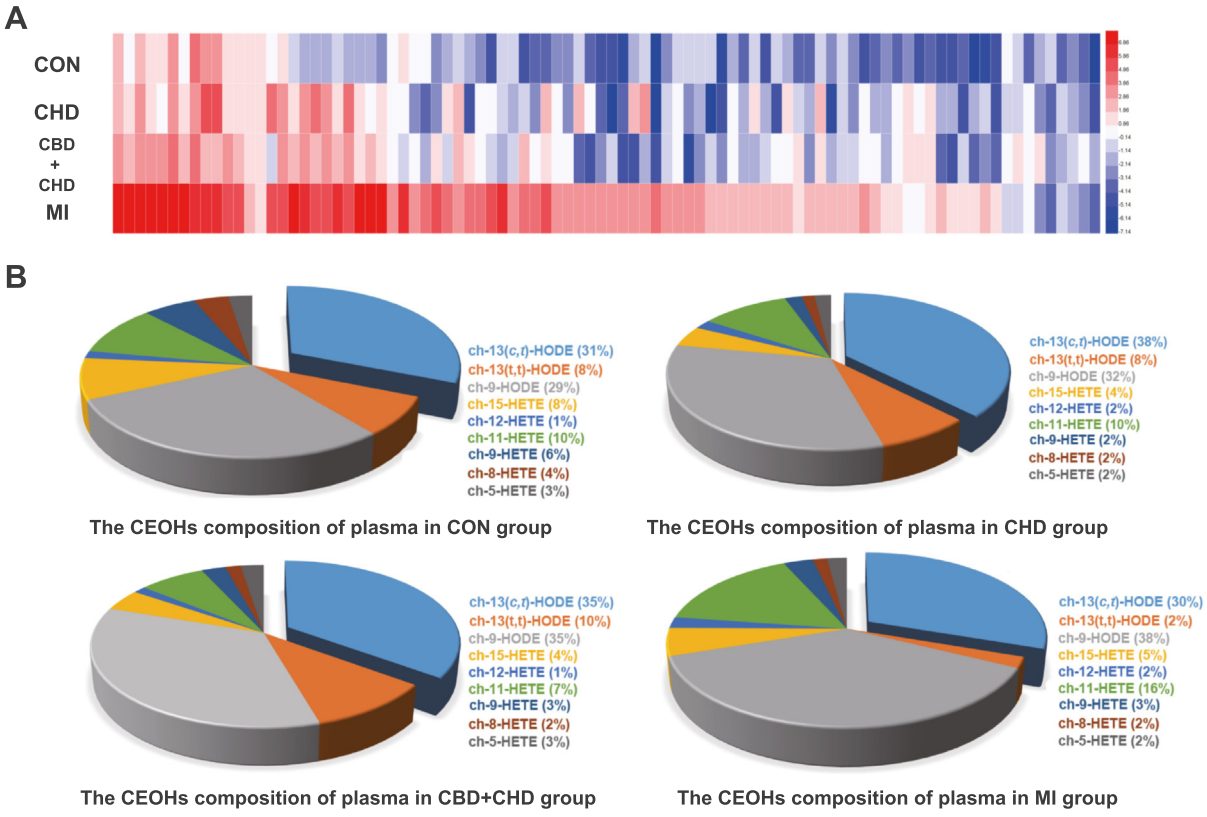

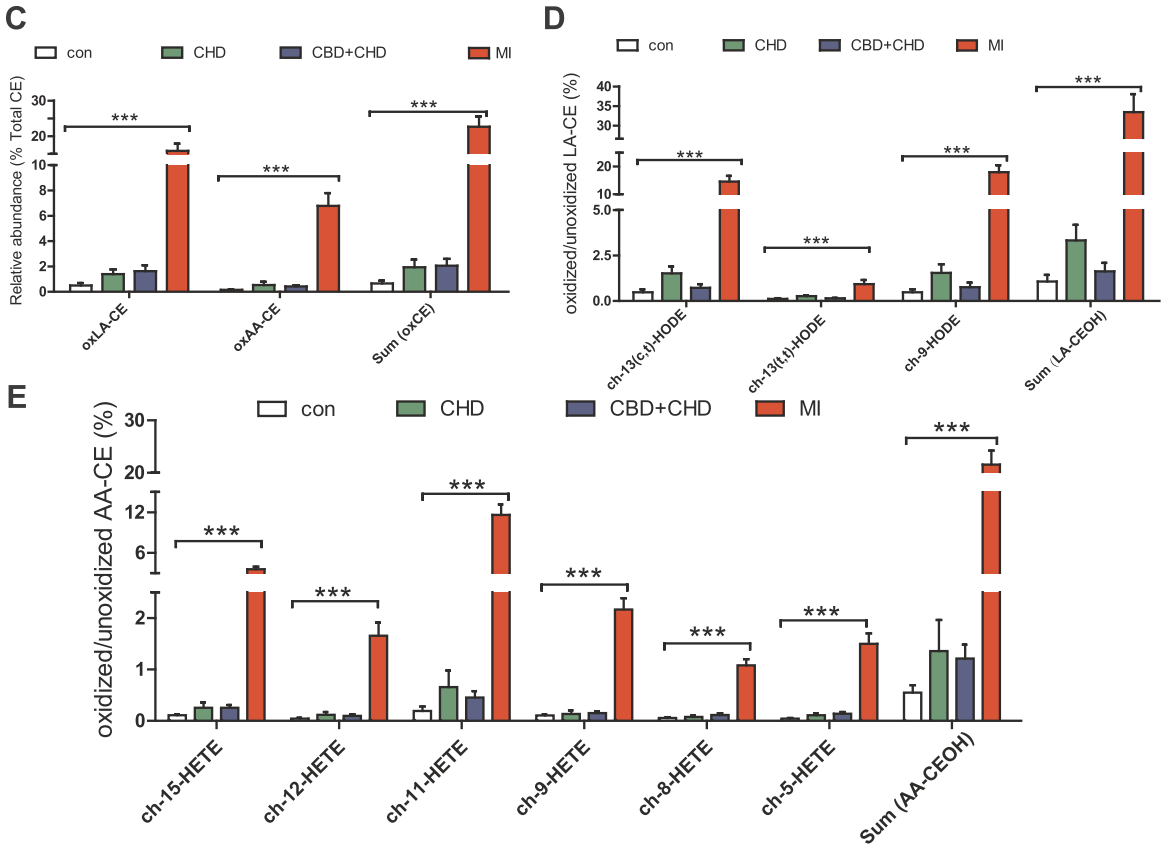

(caption on next page)

Fig. 2. Compositional analysis of oxCEs in human plasma with different CVD. A. Heat maps of the relative amount of CEOHs. (LA-CEOHs and AA-CEOHs) in human plasma (n = 10). Each row represented the CVD groups and each column represented an individual CEOH in each person. Color-coded rectangular cells were relative amount from the logarithmic transformation (log2) of the absolute concentration sorted from high to low: red represented an expression level of CEOHs above mean, blue represented an expression level of CEOHs below the mean. B. The proportion of each oxidized product derived from LA-CE and AA-CE in four groups of human plasma. C. The relative abundance of oxCEs (*versus* total CE) in human plasma samples. D-E. The ratio (%) of oxidized products to un-oxidized products. D represented LA-CE and E represented AA-CE. (B-E, Con: n = 10, CHD: n = 14, CBD + CHD: n = 15, MI: n = 10). Statistical analyses, one-way ANOVA with Bonferroni's test; * ** $p < 0.001$.

significant increase of plasma cholesterol levels while decrease cholesterol levels in liver and macrophages in an LDLR and LXRα-dependent manner.

3.3. Ch-13(c,t)-HpODE induced decrease of LDL and cholesterol uptake in macrophages and hepatocytes

Based on our observation on the cholesterol levels regulated by CEOOH, we hypothesize that the decline of cholesterol levels in liver and peritoneal macrophages is most likely due to the decrease of cholesterol uptake. As shown in Fig. 4, we focused on the effect of ch-13(*c,t*)-HpODE on cholesterol uptake in hepatocytes and macrophages. ch-13(*c,t*)-HpODE significantly decreased cholesterol uptake in primary hepatocytes, whereas the 13(*c,t*)-HpODE, the oxidative product of the free fatty acid, linoleic acid, had no effect on cholesterol uptake (Fig. 4A). In BMDMs, we found that cholesterol uptake was decreased after treating with ch-13(*c,t*)-HpODE, which was similar to a LXRα agonist T09, whereas LA-CE had no effect on cholesterol uptake (Fig. 4B). All these data suggest that esterification of 13-HpODE onto cholesterol (CEOOH) is important in regulating the cholesterol levels. Similarly, the cholesterol uptake was reduced in liver cell line LM3 and macrophage cell line RAW264.7 after treatment with ch-13(*c,t*)-HpODE (Fig. 4C-D). It is noteworthy that the decrease of cholesterol in macrophages may also be caused by the increase of cholesterol efflux. However, we found that the cholesterol efflux was decreased in BMDM and RAW264.7 after treated with ch-13(*c,t*)-HpODE (Supplemental Fig. S4A-B).

Together, all these data demonstrated that the declined cholesterol levels in hepatocytes and macrophages induced by ch-13(*c,t*)-HpODE treatment was due to the decrease of cholesterol uptake.

Our *in vivo* experiments indicated that CEOOH-caused inhibition of cholesterol uptake was dependent on LDLR. To study the role of LDLR pathways in regulation of cholesterol metabolism by CEOOH, we next measured LDL uptake in macrophages and hepatocytes. Consistently, after treating cells with ch-13(*c,t*)-HpODE and GW (a LXRα agonist), LDL uptake was significantly decreased in BMDMs (Fig. 4E and Supplemental Fig. S4C) and LM3 (Fig. 4F).

3.4. The decrease of cholesterol uptake induced by ch-13(c,t)-HpODE was dependent on LXRα-IDOL-LDLR pathway in macrophages both in vivo and in vitro

To test the involvement of LXRα-IDOL-LDLR pathway in CEOOH-regulated cholesterol uptake, we first detected the related gene and protein expressions in peritoneal macrophages. We observed the activation of LXRα and a simultaneous down-regulation of LDLR at protein levels (Fig. 5A). Furthermore, we also observed a dose-dependent increase of *Idol* at mRNA level (Fig. 5B). Therefore, our data are consistent with the hypothesis that the inhibition of cholesterol uptake in macrophages induced ch-13(*c,t*)-HpODE was regulated through LXRα-IDOL-LDLR.

Next, we found that ch-13(*c,t*)-HpODE increased protein levels of LXRα in a time- and dose-dependent manner while decreased LDLR protein level in BMDMs (Fig. 5C-D). As expected, the gene expression of *Idol* was also increased in BMDMs (Fig. 5E) and macrophage cell line RAW264.7 (Fig. 5F) without changing the gene expressions of *Ldlr*. Furthermore, we found that the decrease of LDL uptake induced by ch-13(*c,t*)-HpODE in WT BMDM was abolished in BMDM from $LDLR^{-/-}$ group (Fig. 5G). The decrease of LDLR induced by ch-13(*c,t*)-HpODE in WT BMDM was abolished in BMDMs from $LXR\alpha^{-/-}$ group (Fig. 5H). Consistently, ch-13(*c,t*)-HpODE treatment led to a significant up-regulation of *Idol* at mRNA levels in WT BMDM whereas the changes were significantly attenuated in $LXR\alpha^{-/-}$ group (Fig. 5I). All these data demonstrated that the inhibition of cholesterol uptake induced by ch-13(*c,t*)-HpODE was dependent on LDLR and LXRα *in vitro*.

Interestingly, we found ch-13(*c,t*)-HODE, the reduced form of ch-13(*c,t*)-HpODE, had much weaker effects on cholesterol uptake in BMDM (Supplemental Fig. S5A), consistent with the slight changes of LDLR and LXRα protein expressions (Supplemental Fig. S5B). Furthermore, we also found that the protein expression of LXRβ was slightly increased in BMDMs after treatment with ch-13(*c,t*)-HpODE (Supplemental Fig. S5C).

Taken these data together, ch-13(*c,t*)-HpODE inhibits the cholesterol uptake in macrophages primarily through LXRα-IDOL-LDLR pathways *in vivo* and *in vitro*.

3.5. The inhibitory effects on cholesterol uptake induced ch-13(c,t)-HpODE were due to the decrease of LDLR in liver and hepatocytes

Liver plays very important role in cholesterol metabolism. Next, we examine the effects of CEOOH on liver. In the presence of ch-13(*c,t*)-HpODE, we found a significant increase of LXRα and decrease of LDLR both in liver tissues (Fig. 6A) and primary hepatocytes (Fig. 6B). Similar effects were observed in liver cancer cell lines, LM3 and HepG2 (Fig. 6B). Compared to WT group, the decrease of cholesterol uptake caused by ch-13(*c,t*)-HpODE was significantly attenuated in primary hepatocytes of $LXR\alpha^{-/-}$ (Fig. 6C). These results were similar to the data shown in Fig. 3E, in which the changes of cholesterol level in plasma and liver were dependent on LDLR and LXRα. Notably, previous studies demonstrated that IDOL regulated LDLR expression in a species- and tissue-dependent manner in which mouse hepatic IDOL plays a limited role in modulation of LDLR expression [36]. Even though we observed an increase in IDOL mRNA levels (data not shown), other unknown molecular mechanisms other than IDOL are most likely involved in the regulation of LDLR expression.

In summary, our data strongly suggest that ch-13(*c,t*)-HpODE-induced inhibition of cholesterol uptake is dependent on LXRα and LDLR in liver. However, it remains to be studied the exact molecular mechanisms by which LXRα and LDLR regulate cholesterol uptake in liver in the context of CVD.

4. Discussion

In this study, we employed a targeted lipidomic approach to systematically analyze the oxCE in plasma of CVD patients and found that the levels of various oxidation products are associated with different types of CVD. Interestingly, we observed a significant elevation of multiple oxidation products of LA-CE and AA-CE in plasma of patients with MI compared to control and other CVD groups. Among these oxidation products, ch-13(*c,t*)-HODE is one of the major components that are significantly elevated in plasma of MI patients. We independently synthesized ch-13(*c,t*)-HpODE, the primary oxidation products of LA-CE in LDL, to study their biological effects on cholesterol metabolism in the context of CVD. We found that the low doses of ch-

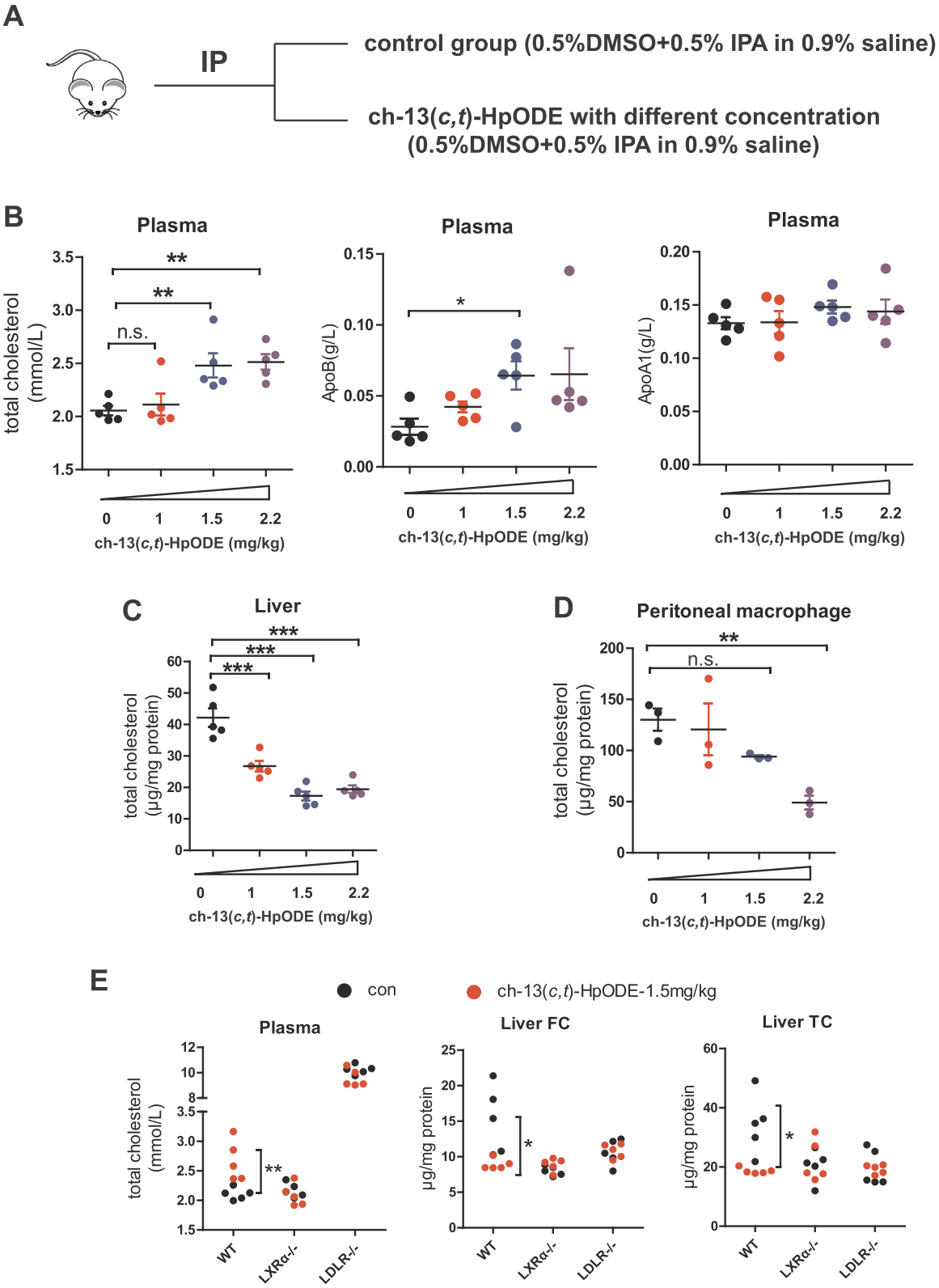

Fig. 3. The effects of ch-13(*c,t*)-HpODE on cholesterol levels *in vivo*. A. The experimental procedure of ch-13(*c,t*)-HpODE treatment *in vivo*. B. Total cholesterol, ApoB and ApoA1 were detected in mice plasma (Duplicates and n = 5) after treating mice with ch-13(*c,t*)-HpODE. C-D. Total cholesterol was detected with GC-MS in liver (C, n = 5) and peritoneal macrophages (D, 3 repeats per experiment) after treating mice with ch-13(*c,t*)-HpODE. E. Free or total cholesterol was detected in plasma and liver after treating WT, LXRα-/-and LDLR-/- mice with 1.5 mg/kg ch-13(*c,t*)-HpODE (n = 5, 3 independent experiments). FC: Free cholesterol; TC: Total cholesterol; n.s.: no significance. Statistical analyses, one-way ANOVA with Dunnett's test or two-way ANOVA and unpaired *t*-test. $^{*}p < 0.05$, $^{**}p < 0.01$, $^{***}p < 0.001$.

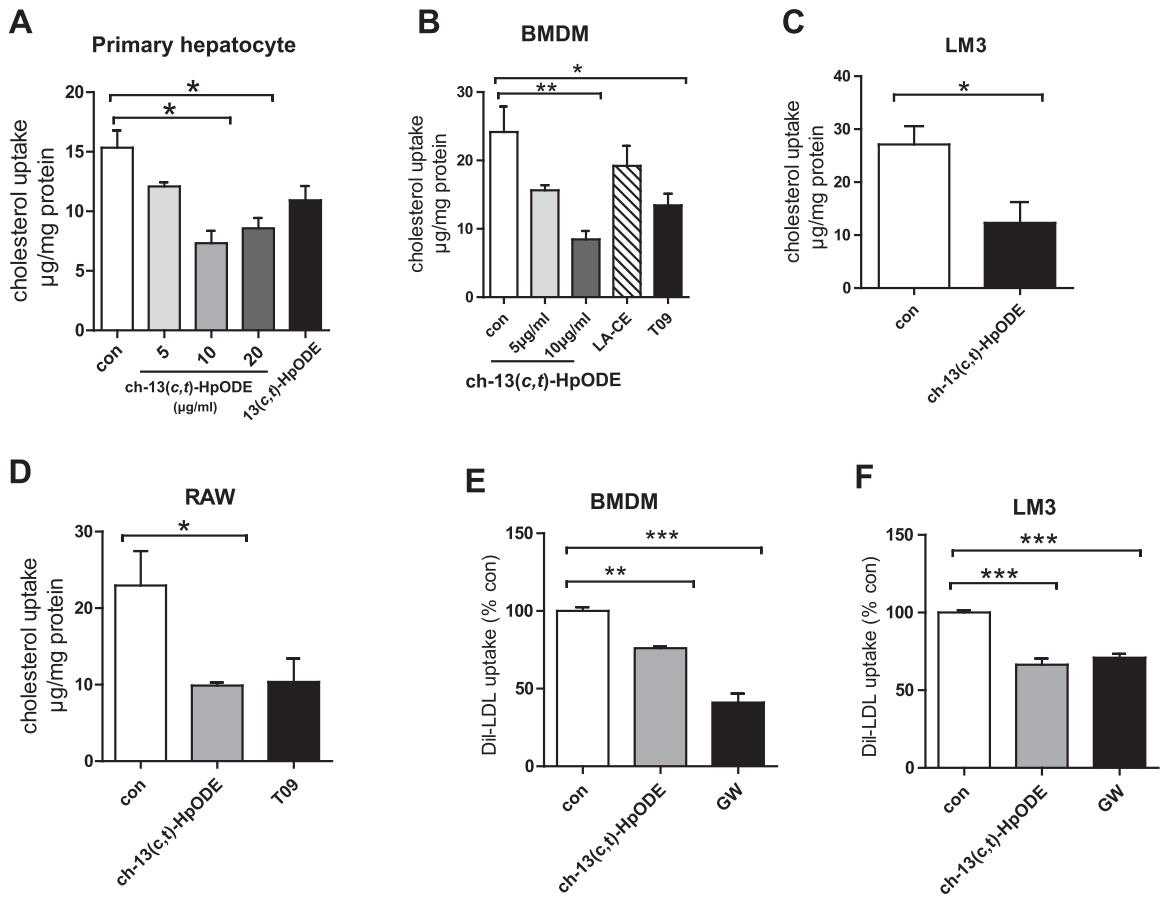

Fig. 4. Ch-13(*c,t*)-HpODE decreased the uptake of cholesterol and LDL *in vitro*. Cholesterol uptake assay (A-D): cells were stimulated with different compounds for 24 h in the presence of 25 μg/ml LDL and 15 μg/ml chol-d7. Total chol-d7 was quantified in cells by GC-MS. A-B. The cholesterol uptake in primary hepatocytes (A) and BMDMs (B). LA-CE (10 μg/ml), T09 (positive control, 5 μM). 13(*c,t*)-HpODE(14 μM). C-D. The cholesterol uptake in LM3 (C) and RAW264.7 (D). Ch-13(*c,t*)-HpODE (10 μg/ml), T09 (10 μM). E-F. LDL uptake: BMDMs (E) and LM3 (F) were treated with control, 10 μg/ml ch-13(*c,t*)-HpODE, 2 μM GW (positive control) for 24 h. After washing with PBS, 20 μg/ml Dil-LDL were added and incubated for another 8 h in 37 °C before the cells were washed and fixed for Dil-LDL uptake assay. Con: control. Data are expressed as the mean ± SEM. and representative of ≥ 3 independent experiments. Statistical analyses, one-way ANOVA with Dunnett's test (B,D-F) and unpaired *t*-test (A,C). $*p < 0.05$, $**p < 0.01$, $***p < 0.001$.

13(*c,t*)-HpODE significantly increased the cholesterol levels in mice plasma and decreased the cholesterol level in liver and peritoneal macrophages. In macrophages, the decrease of cholesterol uptake induced by ch-13(*c,t*)-HpODE was dependent on LXRα-IDOL-LDLR pathway. In liver, the inhibitory effects of CEOOH on cholesterol uptake were dependent on LDLR and LXRα (Fig. 7). Our studies suggest that the levels of oxCE in human plasma might serve as a potential biomarker for different types of CVD, especially for MI. Furthermore, the regulation of cholesterol levels by oxCE represents a novel molecular mechanism by which cholesterol levels are modulated *in vivo* in the context of CVD.

Overwhelming evidence has demonstrated that oxLDL plays a significant role in atherosclerosis and CVD [7,37,38]. Free radical-induced lipid peroxidation of PUFAs in LDL is a complicated process and tremendous research efforts have been devoted to characterize these oxidation products and study their biological relevance in CVD [8,9,13]. Harland et al. reported the presence of LA-CEOOHs in atherosclerotic plaques of human aortas by GC-MS [39]. Later studies found that more isomers of LA-CEOHs in plasma from healthy humans [40] and in advanced atherosclerotic lesions [11]. With the development of mass spectrometry (MS), more oxidized products from LA-CEs and AA-CEs have been isolated and detected in human lesions [12] as well as in filter samples after peripheral arterial interventions [41]. Our previous studies systematically identified oxidation products of LA-CE and AA-CE based on MS techniques [10]. However, the associations of oxCEs in plasma of patients with different types of CVD remain to be established. In this study, we developed a targeted lipidomic approach to quantify multiple classes of oxCE and observed a positive association between levels of oxidation products of LA-CE and AA-CE in plasma with MI (Fig. 1). These results are consistent with our previous reports that lipid peroxidation is a prominent feature in plasma from patients with CVD [38]. Furthermore, the LA-CEOHs accounted for 70% of oxidation products and the levels of LA-CEOHs in MI group were significantly higher than those in control group (Figs. 1 and 2). These results were similar to previously reports in which CEOHs (18:2) was the most oxidation products in human plaques followed by AA-CEOHs [12]. Once validated in larger clinical cohorts in future studies, the profiles of oxCE in human plasma have the potential to become a biomarker for MI. Interestingly, the levels of oxCE are much higher than those of well-studied oxysterols reported in the literature [4]. A majority of the oxCE are derived from lipid peroxidation under oxidative stress, whereas most oxysterols are produced from cytochrome P450. These two classes of sterol metabolites are likely play important yet different roles in the settings of CVD.

Biological activities of oxLDL in atherosclerosis and CVD have been thus far mainly focused on the inflammatory responses in macrophages, endothelial cells, and platelets [6]. Previous studies demonstrated that minimally modified LDL (mmLDL) promoted atherosclerosis through cytoskeleton changes [42], lipid accumulation [43], ROS generation [44], and inflammatory response in macrophages [45,46]. Surprisingly,

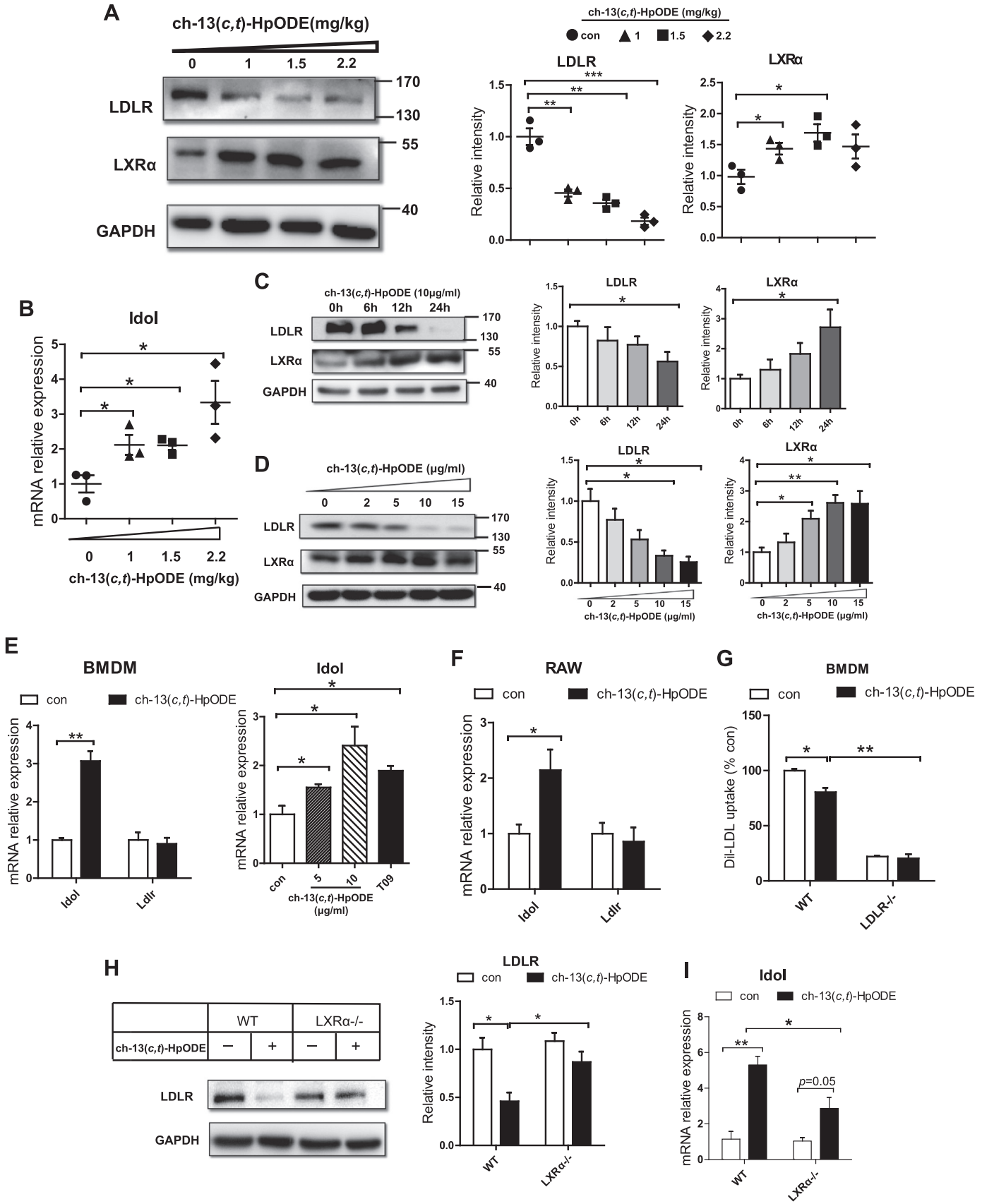

(caption on next page)

Fig. 5. ch-13(*c,t*)-HpODE decreased the cholesterol uptake in macrophages *via* LXRα-IDOL-LDLR pathway. A-B. The protein expression (A) and gene expression (B) in peritoneal macrophages after treating mice with ch-13(*c,t*)-HpODE. C-D. BMDMs were treated with different time (C) and concentration (D) of ch-13(*c,t*)-HpODE and protein levels of LDLR and LXRα were analyzed by Western blot. E-F. The gene expression of BMDMs (E) and RAW 264.7 (F) after treating with ch-13(*c,t*)-HpODE for 24 h. G. After treating with ch-13(*c,t*)-HpODE for 24 h, 20 μg/ml Dil-LDL were added for another 8 h in 37 °C, Dil-LDL uptake was measured in BMDM from WT and LDLR-/- mice. H-I. After treating with ch-13(*c,t*)-HpODE for 24 h, the protein expression (H) and gene expression (I) were measured in BMDMs from WT and LXRα-/- mice. Con: control. Data are expressed as the mean ± SEM. and representative of ≥ 3 independent experiments in duplicate (A-B, E-F, H-I) or ≥ 3 independent experiments (C-D,G). Statistical analyses, unpaired *t*-test (A, B, C-F) and two way ANOVA (G-I). $*p < 0.05$, $**p < 0.01$, $***p < 0.001$.

however, the roles of these oxidation products on cholesterol metabolism is much less studied despite the fact that dysregulation of cholesterol homeostasis causes CVD. To dissect the biological activities of oxCE, we purified ch-13(*c,t*)-HpODE derived from LA-CE and used it as a representative for CEOOHs. Even though we detected more ch-13(*c,t*)-HODE in human plasma, previous studies have demonstrated that the reduced form of lipid hydroperoxides were much less bioactive compared to their hydroperoxides [33,34]. A body of evidence suggests that CEOOHs are generated in different tissues where they exert their biological functions before they are reduced and released into the blood stream. Therefore we choose ch-13(*c,t*)-HpODE as a representative of CEOOHs to explore its effects on cholesterol metabolism.

As an important class of immune cells, macrophages are critical for cholesterol metabolism, such as cholesterol synthesis, uptake, and efflux. Previous studies found that mmLDL changed cytoskeleton and promoted lipid accumulation in macrophages. Harkewicz *et al.* demonstrated that oxAA-CEs were the components of mmLDL and promoted lipid accumulation and immune response in macrophages [33]. Bicyclic endoperoxide and hydroperoxide (BEP-CE) derived from AA-CEOOH induced the activation of macrophages *via* Toll like receptor 4 (TLR4) and spleen tyrosine kinase (SYK) [6,47]. Our current study demonstrated that ch-13(*c,t*)-HpODE decreased cholesterol and LDL uptake in macrophages (Fig. 4). Recent studies illustrated that the increase of plasma cholesterol levels was due to the decrease of LDL uptake, which is regulated by LXR-IDOL-LDLR pathway [16]. In our study, we also found that these endogenous CEOOH decreased cholesterol uptake in macrophages *via* activating LXRα-IDOL-LDLR axis (Figs. 4 and 5). And we also found LDLR and LXR were essential to the inhibition of cholesterol uptake induced by ch-13(*c,t*)-HpODE (Fig. 4). Notably, we also found that CEOOHs increased the expression of LXRβ

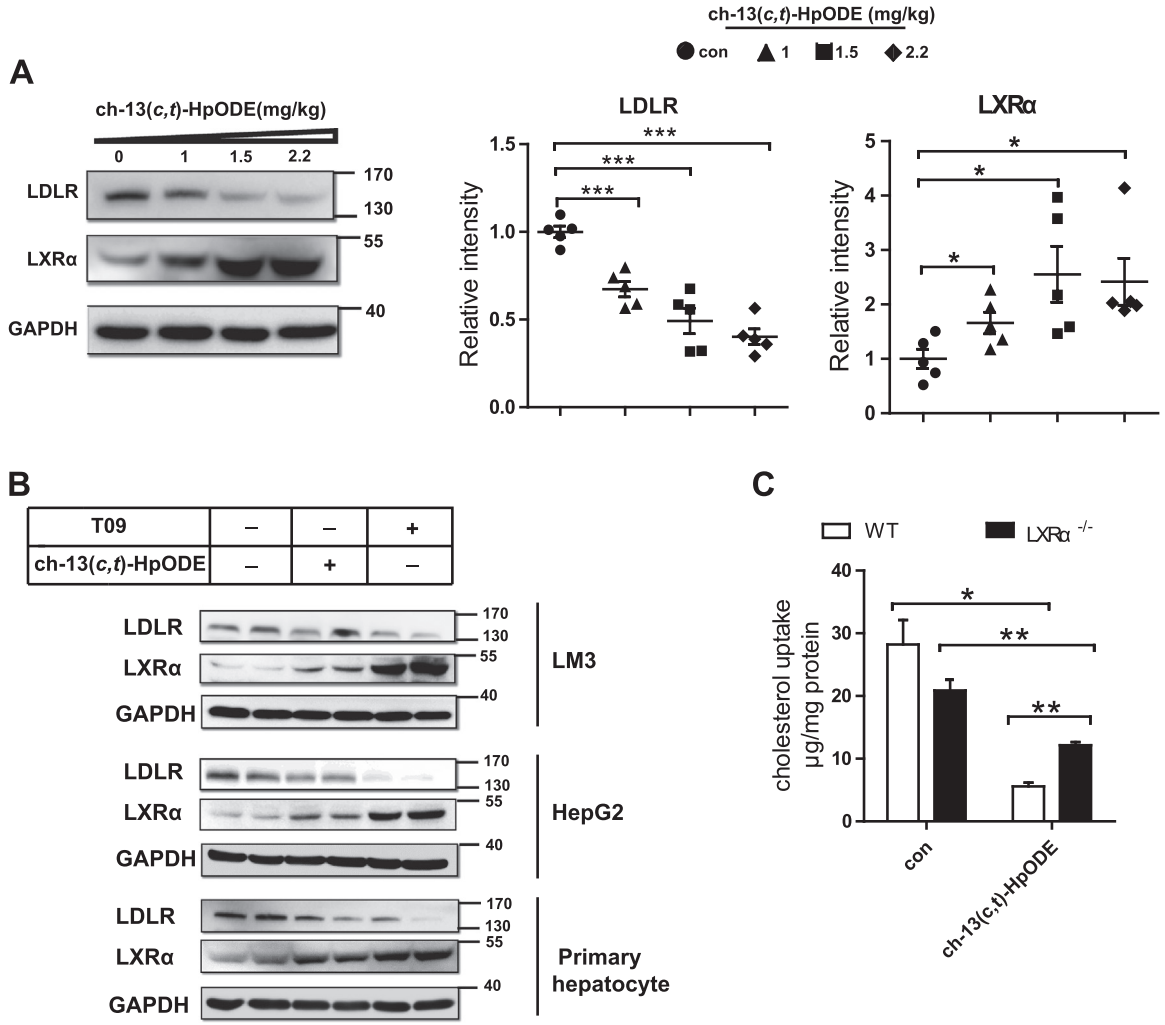

Fig. 6. The inhibitory effects of ch-13(*c,t*)-HpODE on cholesterol uptake were dependent on LXRα and LDLR in liver and hepatocytes. A. The LDLR and LXRα protein expression in liver tissues after injection of WT mice with ch-13(*c,t*)-HpODE (n = 5, 3 independent experiments). B. Primary hepatocytes, HepG2 and LM3 were stimulated with con, 10 μg/ml ch-13(*c,t*)-HpODE, T09 (5 μM) for 24 h before the cell lysates were analyzed by Western blot (3 independent experiments in duplicate). C. Cholesterol uptake was measured in primary hepatocytes from WT and LXRα-/- after treating with control and 10 μg/ml ch-13(*c,t*)-HpODE for 24 h (3 independent experiments). Con: control. Statistical analyses, two-way ANOVA and unpaired *t*-test. $*p < 0.05$, $**p < 0.01$, $***p < 0.001$.

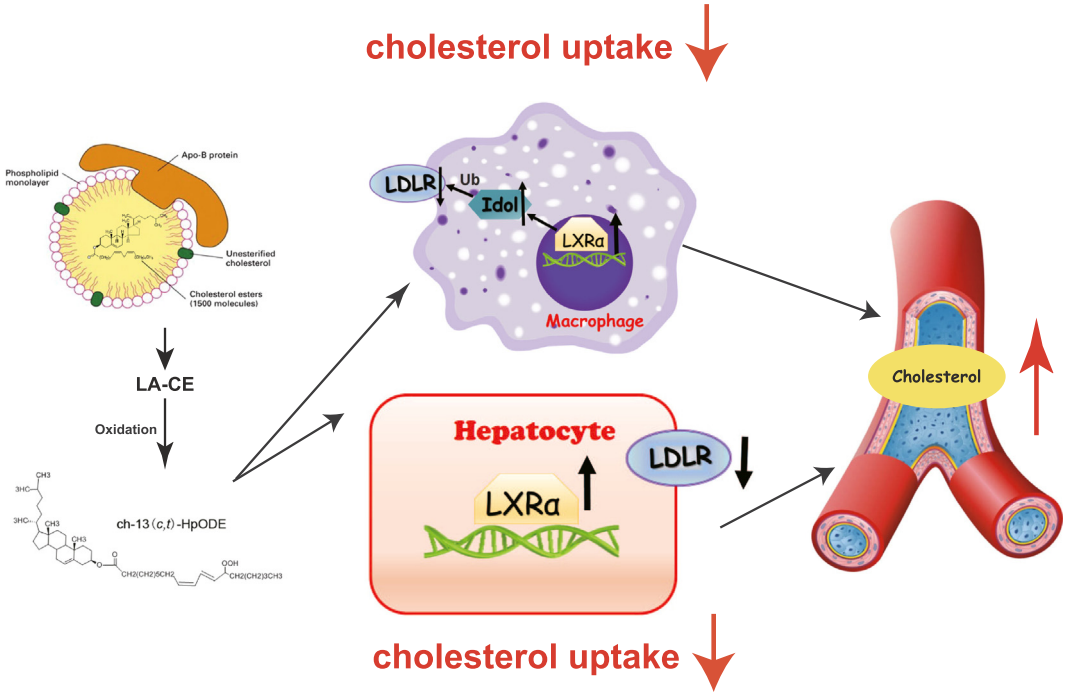

Fig. 7. Cholesterol ester hydroperoxides derived from oxidized LDL regulate cholesterol levels in plasma, macrophages and hepatocytes. Polyunsaturated fatty acids containing-CEs in LDL can be oxidized by ROS to generate CEOOHs. As one of the most abundant CEOOHs in LDL, ch-13(*c,t*)-HpODE increases plasma cholesterol levels and inhibits cholesterol uptake of macrophages and hepatocytes. In macrophages, ch-13(*c,t*)-HpODE activates LXRα-IDOL-LDLR pathway, whereas in hepatocytes, the inhibition of cholesterol uptake is dependent on LDLR and LXRα.

in macrophages (Supplemental Fig. S5C), consistent with the slight increase of *Idol* in LXRα$^{-/-}$ group (Fig. 5I).

Liver plays a critical role in cholesterol and LDL metabolism. As a critical regulator of cholesterol uptake to maintain cholesterol level in the blood circulation, LDLR is regulated by LXR, PCSK9 (proprotein convertase subtilisin/kexin type 9 serine protease gene) and SREBP (sterol regulator sterol regulatory element–binding protein) [48,49]. In this study, we found that ch-13(*c,t*)-HpODE decreased cholesterol levels in the liver, which has been primarily attributed to the decreased cholesterol uptake in hepatocyte (Figs. 3 and 4). Furthermore, CEOOHs decreases cholesterol uptake *via* down-regulating LDLR (Fig. 6), which is also dependent on LXRα both *in vivo* and *in vitro* (Figs. 3 and 6). Intriguingly, however, previous studies suggest that the protein expression of LDLR was not regulated by LXRα-IDOL pathway in mouse liver [36]. It remains to be studied how LXRα and LDLR are involved in the regulation of cholesterol levels and uptake in the liver in the context of CVD.

Our current study demonstrated that inhibition of cholesterol uptake by ch-13(*c,t*)-HpODE in macrophages is dependent on LXRα-IDOL-LDLR pathway, whereas inhibition of cholesterol levels in hepatocytes was dependent on LXRα and LDLR. LXRα is a critical regulator of cholesterol metabolism including cholesterol uptake, efflux, secretion, and absorption [50,51]. However, it remains unclear how LXR is activated *in vivo*. In this study, the oxidation of these PUFA-containing CE by free radical lipid peroxidation leads to the increase of LXRα both in macrophages and liver (Figs. 5 and 6). Our preliminary experiments found that CEOOHs increased the protein expression of LXRα through inhibiting the ubiquitination and degradation without affecting the transcriptional activities (data not shown). Furthermore, we found that some of the target genes of LXRα were increased in the liver, such as *Abca1*, *Abcg5*, *Abcg8* (Supplemental Fig. S6A). Interestingly, the cholesterol level was also increased in feces after treating mice with ch-13(*c,t*)-HpODE (Supplemental Fig. S6B), suggesting that increased cholesterol excretion also contributed to the decrease of cholesterol in liver, consistent with the increased expression of *Abcg5* and *Abcg8*. All these data suggest that multiple mechanisms are likely involved in the decrease of cholesterol in liver induced by CEOOHs, among which cholesterol uptake plays an important role. Our observations laid the ground for further molecular studies related to the effects on cholesterol metabolism in liver caused by CEOOHs.

In summary, our study reveals that CEOOHs increase circulating cholesterol levels while decrease cholesterol levels in the liver and macrophages. Furthermore, the inhibition of cholesterol uptake was due to the activation of LXRα-IDOL-LDLR in macrophage, whereas in hepatocytes, CEOOHs can also decrease LDLR to inhibit cholesterol uptake. Together, our study identified a novel mechanism by which endogenous oxCE in oxLDL contributes to the pathogenesis of CVD. The impact of this mechanism warrants further study in the context of CVD. On the one hand, increased plasma cholesterol levels represents a major risk factor for CVD. On the other hand, decreased cholesterol uptake in macrophages may lead to the decreased foam cell formation, which appears to be beneficial for CVD. However, oxidized lipids can be taken up by other scavenger receptors, such as CD36, to induce foam cell formation. Thus, it remains to be studied how this mechanism identified in this study is related to atherosclerosis. Meanwhile, CEOOHs were significantly increased in patients with MI. It warrants future studies to investigate if these oxidation products contribute to MI or significant elevation of these compounds is just a consequence of MI due to post-ischemic oxidative stress combined with uncontrolled clog rupture. Moreover, future research attentions need to be paid to the gender difference of these oxCE and the correlations of these oxidation products to the known clinical variables related to CVDs.

Acknowledgements

We acknowledge the constructive discussions with Dr. Peter Tontonoz at University of California at Los Angeles on the LXR-IDOL-LDLR pathways. We thank Dr. Ben He at the Renji Hospital affiliated with Shanghai Jiao Tong University for providing with the LXRα KO mice. A stimulating discussion with Drs. Yuri Miller and Sotirios

Tsimikas at University of California at San Diego is also appreciated.

Sources of funding

This work was financially supported by the National Key R&D Program of China administered by Chinese Ministry of Science and Technology (MOST) (2016YFC0903403 and 2016YFD0400205), National Natural Science Foundation of China (31470831, 91439103, 91539127, 31401015 and 9185112), and the Chinese Academy of Sciences (ZDBS-SSW-DQC-02).

Disclosures

None.

Appendix A. Supplementary material

Supplementary data associated with this article can be found in the online version at doi:10.1016/j.redox.2018.101069.

References

[1] B. Cannon, Biochemistry to behaviour, Nature 493 (2013) S2–S3.
[2] W.H. Tang, S.L. Hazen, Atherosclerosis in 2016: advances in new therapeutic targets for atherosclerosis, Nat. Rev. Cardiol. 14 (2017) 71–72.
[3] A.J. Brown, W. Jessup, Oxysterols: sources, cellular storage and metabolism, and new insights into their roles in cholesterol homeostasis, Mol. Asp. Med. 30 (2009) 111–122.
[4] G.J. Schroepfer Jr., Oxysterols: modulators of cholesterol metabolism and other processes, Physiol. Rev. 80 (2000) 361–554.
[5] B.A. Ference, H.N. Ginsberg, I. Graham, K.K. Ray, C.J. Packard, E. Bruckert, R.A. Hegele, R.M. Krauss, F.J. Raal, H. Schunkert, G.F. Watts, J. Boren, S. Fazio, J.D. Horton, L. Masana, S.J. Nicholls, B.G. Nordestgaard, B. van de Sluis, M.R. Taskinen, L. Tokgozoglu, U. Landmesser, U. Laufs, O. Wiklund, J.K. Stock, M.J. Chapman, A.L. Catapano, Low-density lipoproteins cause atherosclerotic cardiovascular disease. 1. Evidence from genetic, epidemiologic, and clinical studies. A consensus statement from the European Atherosclerosis Society Consensus Panel, Eur. Heart J. 38 (2017) 2459–2472.
[6] S.H. Choi, D. Sviridov, Y.I. Miller, Oxidized cholesteryl esters and inflammation, Biochim. Biophys. Acta 1862 (2017) 393–397.
[7] J. Lu, S. Guo, X. Xue, Q. Chen, J. Ge, Y. Zhuo, H. Zhong, B. Chen, M. Zhao, W. Han, T. Suzuki, M. Zhu, L. Xia, C. Schneider, T.S. Blackwell, N.A. Porter, L. Zheng, S. Tsimikas, H. Yin, Identification of a novel series of anti-inflammatory and anti-oxidative phospholipid oxidation products containing the cyclopentenone moietyin vitroandin vivo: implication in atherosclerosis, J. Biol. Chem. 292 (2017) 5378–5391.
[8] S. Lee, K.G. Birukov, C.E. Romanoski, J.R. Springstead, A.J. Lusis, J.A. Berliner, Role of phospholipid oxidation products in atherosclerosis, Circ. Res. 111 (2012) 778–799.
[9] H. Yin, L. Xu, N.A. Porter, Free radical lipid peroxidation: mechanisms and analysis, Chem. Rev. 111 (2011) 5944–5972.
[10] H. Yin, C.M. Havrilla, J.D. Morrow, N.A. Porter, Formation of isoprostane bicyclic endoperoxides from the autoxidation of cholesteryl arachidonate, J. Am. Chem. Soc. 124 (2002) 7745–7754.
[11] J.M. Upston, X.W. Niu, A.J. Brown, R. Mashima, H.J. Wang, R. Senthilmohan, A.J. Kettle, R.T. Dean, R. Stocker, Disease stage-dependent accumulation of lipid and protein oxidation products in human atherosclerosis, Am. J. Pathol. 160 (2002) 701–710.
[12] P.M. Hutchins, E.E. Moore, R.C. Murphy, Electrospray MS/MS reveals extensive and nonspecific oxidation of cholesterol esters in human peripheral vascular lesions, J. Lipid Res. 52 (2011) 2070–2083.
[13] N. Leitinger, Cholesteryl ester oxidation products in atherosclerosis, Mol. Asp. Med. 24 (2003) 239–250.
[14] J.L. Goldstein, M.S. Brown, A century of cholesterol and coronaries: from plaques to genes to statins, Cell 161 (2015) 161–172.
[15] F. Bovenga, C. Sabba, A. Moschetta, Uncoupling nuclear receptor LXR and cholesterol metabolism in cancer, Cell Metab. 21 (2015) 517–526.
[16] L. Zhang, K. Reue, L.G. Fong, S.G. Young, P. Tontonoz, Feedback regulation of cholesterol uptake by the LXR-IDOL-LDLR axis, Arterioscler. Thromb. Vasc. Biol. 32 (2012) 2541–2546.
[17] S.D. Lee, P. Tontonoz, Liver X receptors at the intersection of lipid metabolism and atherogenesis, Atherosclerosis 242 (2015) 29–36.
[18] N. Zelcer, C. Hong, R. Boyadjian, P. Tontonoz, LXR regulates cholesterol uptake through Idol-dependent ubiquitination of the LDL receptor, Science 325 (2009) 100–104.
[19] N. Tanaka, T. Aoyama, S. Kimura, F.J. Gonzalez, Targeting nuclear receptors for the treatment of fatty liver disease, Pharmacol. Ther. 179 (2017) 142–157.
[20] S. Guo, L. Li, H. Yin, Cholesterol homeostasis and liver X receptor (LXR) inAtherosclerosis, Cardiovasc. Hematol. Disord. Drug Targets 18 (2018) 27–33.
[21] C. Punta, C.L. Rector, N.A. Porter, Peroxidation of polyunsaturated fatty acid methyl esters catalyzed by N-methyl benzohydroxamic acid: a new and convenient method for selective synthesis of hydroperoxides and alcohols, Chem. Res. Toxicol. 18 (2005) 349–356.
[22] Q. He, J. Pu, A. Yuan, W.B. Lau, E. Gao, W.J. Koch, X.L. Ma, B. He, Activation of liver-X-receptor alpha but not liver-X-receptor beta protects against myocardial ischemia/reperfusion injury, Circ. Heart Fail. 7 (2014) 1032–1041.
[23] L.M. Pei, H. Waki, B. Vaitheesvaran, D.C. Wilpitz, I.J. Kurland, P. Tontonoz, NR4A orphan nuclear receptors are transcriptional regulators of hepatic glucose metabolism, Nat. Med. 12 (2006) 1048–1055.
[24] M. Ouimet, H.N. Ediriweera, U.M. Gundra, F.J. Sheedy, B. Ramkhelawon, S.B. Hutchison, K. Rinehold, C. van Solingen, M.D. Fullerton, K. Cecchini, K.J. Rayner, G.R. Steinberg, P.D. Zamore, E.A. Fisher, P. Loke, K.J. Moore, MicroRNA-33-dependent regulation of macrophage metabolism directs immune cell polarization in atherosclerosis, J. Clin. Investig. 125 (2015) 4334–4348.
[25] H. Yin, B.E. Cox, W. Liu, N.A. Porter, J.D. Morrow, G.L. Milne, Identification of intact oxidation products of glycerophospholipids in vitro and in vivo using negative ion electrospray iontrap mass spectrometry, J. Mass Spectrom. 44 (2009) 672–680.
[26] W. Liu, H. Yin, Y.O. Akazawa, Y. Yoshida, E. Niki, N.A. Porter, Ex vivo oxidation in tissue and plasma assays of hydroxyoctadecadienoates: Z,E/E,E stereoisomer ratios, Chem. Res. Toxicol. 23 (2010) 986–995.
[27] Y.-J. Wang, Y. Bian, J. Luo, M. Lu, Y. Xiong, S.-Y. Guo, H.-Y. Yin, X. Lin, Q. Li, C.C.Y. Chang, T.-Y. Chang, B.-L. Li, B.-L. Song, Cholesterol and fatty acids regulate cysteine ubiquitylation of ACAT2 through competitive oxidation, Nat. Cell Biol. 19 (2017) 808–819.
[28] C.M. Havrilla, D.L. Hachey, N.A. Porter, Coordination (Ag+) ion spray-mass spectrometry of peroxidation products of cholesterol linoleate and cholesterol arachidonate: high-performance liquid chromatography-mass spectrometry analysis of peroxide products from polyunsaturated lipid autoxidation, J. Am. Chem. Soc. 122 (2000) 8042–8055.
[29] Y. Kawai, M. Miyoshi, J.H. Moon, J. Terao, Detection of cholesteryl ester hydroperoxide isomers using gas chromatography-mass spectrometry combined with thin-layer chromatography blotting, Anal. Biochem. 360 (2007) 130–137.
[30] E. Rigamonti, L. Helin, S. Lestavel, A.L. Mutka, M. Lepore, C. Fontaine, M.A. Bouhlel, S. Bultel, J.C. Fruchart, E. Ikonen, V. Clavey, B. Staels, G. Chinetti-Gbaguidi, Liver X receptor activation controls intracellular cholesterol trafficking and esterification in human macrophages, Circ. Res. 97 (2005) 682–689.
[31] P. Robinet, Z. Wang, S.L. Hazen, J.D. Smith, A simple and sensitive enzymatic method for cholesterol quantification in macrophages and foam cells, J. Lipid Res. 51 (2010) 3364–3369.
[32] J.A. Kenar, C.M. Havrilla, N.A. Porter, J.R. Guyton, S.A. Brown, K.R. Klemp, E. Selinger, Identification and quantification of the regioisomeric cholesteryl linoleate hydroperoxides in oxidized human low density lipoprotein and high density lipoprotein, Chem. Res. Toxicol. 9 (1996) 737–744.
[33] R. Harkewicz, K. Hartvigsen, F. Almazan, E.A. Dennis, J.L. Witztum, Y.I. Miller, Cholesteryl ester hydroperoxides are biologically active components of minimally oxidized low density lipoprotein, J. Biol. Chem. 283 (2008) 10241–10251.
[34] J. Huber, H. Boechzelt, B. Karten, M. Surboeck, V.N. Bochkov, B.R. Binder, W. Sattler, N. Leitinger, Oxidized cholesteryl linoleates stimulate endothelial cells to bind monocytes via the extracellular signal-regulated kinase 1/2 pathway, Arter. Throm. Vas. 22 (2002) 581–586.
[35] H. Itabe, M. Mori, Y. Fujimoto, Y. Higashi, T. Takano, Minimally modified LDL is an oxidized LDL enriched with oxidized phosphatidylcholines, J. Biochem. 134 (2003) 459–465.
[36] C. Hong, S.M. Marshall, A.L. McDaniel, M. Graham, J.D. Layne, L. Cai, E. Scotti, R. Boyadjian, J. Kim, B.T. Chamberlain, R.K. Tangirala, M.E. Jung, L. Fong, R. Lee, S.G. Young, R.E. Temel, P. Tontonoz, The LXR-Idol axis differentially regulates plasma LDL levels in primates and mice, Cell Metab. 20 (2014) 910–918.
[37] D. Steinberg, J.L. Witztum, Oxidized low-density lipoprotein and atherosclerosis, Arterioscler. Thromb. Vasc. Biol. 30 (2010) 2311–2316.
[38] J.H. Lu, B.X. Chen, T.T. Chen, S.Y. Guo, X.L. Xue, Q. Chen, M.M. Zhao, L. Xia, Z.J. Zhu, L.M. Zheng, H.Y. Yin, Comprehensive metabolomics identified lipid peroxidation as a prominent feature in human plasma of patients with coronary heart diseases, Redox Biol. 12 (2017) 899–907.
[39] W.A. Harland, J.D. Gilbert, C.J.W. Brooks, Lipids of human atheroma. 8. Oxidized derivatives of cholesteryl linoleate, Biochim. Biophys. Acta 316 (1973) 378–385.
[40] R. Mashima, K. Onodera, Y. Yamamoto, Regioisomeric distribution of cholesteryl linoleate hydroperoxides and hydroxides in plasma from healthy humans provides evidence for free radical-mediated lipid peroxidation in vivo, J. Lipid Res. 41 (2000) 109–115.
[41] A. Ravandi, G. Leibundgut, M.Y. Hung, M. Patel, P.M. Hutchins, R.C. Murphy, A. Prasad, E. Mahmud, Y.I. Miller, E.A. Dennis, J.L. Witztum, S. Tsimikas, Release and capture of bioactive oxidized phospholipids and oxidized cholesteryl esters during percutaneous coronary and peripheral arterial interventions in humans, J. Am. Coll. Cardiol. 63 (2014) 1961–1971.
[42] Y.I. Miller, S. Viriyakosol, C.J. Binder, J.R. Feramisco, T.N. Kirkland, J.L. Witztum, Minimally modified LDL binds to CD14, induces macrophage spreading via TLR4/MD-2, and inhibits phagocytosis of apoptotic cells, J. Biol. Chem. 278 (2003) 1561–1568.
[43] S.H. Choi, R. Harkewicz, J.H. Lee, A. Boullier, F. Almazan, A.C. Li, J.L. Witztum, Y.S. Bae, Y.I. Miller, Lipoprotein accumulation in macrophages via toll-like receptor-4-dependent fluid phase uptake, Circ. Res. 104 (2009) 1355–1363.
[44] Y.S. Bae, J.H. Lee, S.H. Choi, S. Kim, F. Almazan, J.L. Witztum, Y.I. Miller, Macrophages generate reactive oxygen species in response to minimally oxidized low-density lipoprotein: toll-like receptor 4- and spleen tyrosine kinase-dependent

activation of NADPH oxidase 2, Circ. Res. 104 (2009) 210–218 (221p following 218).
[45] P. Wiesner, S.H. Choi, F. Almazan, C. Benner, W. Huang, C.J. Diehl, A. Gonen, S. Butler, J.L. Witztum, C.K. Glass, Y.I. Miller, Low doses of lipopolysaccharide and minimally oxidized low-density lipoprotein cooperatively activate macrophages via nuclear factor kappa B and activator protein-1 possible mechanism for acceleration of atherosclerosis by subclinical endotoxemia, Circ. Res. 107 (2010) 56–65.
[46] Y.I. Miller, S. Viriyakosol, D.S. Worrall, A. Boullier, S. Butler, J.L. Witztum, Toll-like receptor 4-dependent and -independent cytokine secretion induced by minimally oxidized low-density lipoprotein in macrophages, Arterioscler. Thromb. Vasc. Biol. 25 (2005) 1213–1219.
[47] S.H. Choi, H. Yin, A. Ravandi, A. Armando, D. Dumlao, J. Kim, F. Almazan, A.M. Taylor, C.A. McNamara, S. Tsimikas, E.A. Dennis, J.L. Witztum, Y.I. Miller, Polyoxygenated cholesterol ester hydroperoxide activates TLR4 and SYK dependent signaling in macrophages, PLoS One 8 (2013) e83145.
[48] L. Goedeke, N. Rotllan, A. Canfran-Duque, J.F. Aranda, C.M. Ramirez, E. Araldi, C.S. Lin, N.N. Anderson, A. Wagschal, R. de Cabo, J.D. Horton, M.A. Lasuncion, A.M. Naar, Y. Suarez, C. Fernandez-Hernando, MicroRNA-148a regulates LDL receptor and ABCA1 expression to control circulating lipoprotein levels, Nat. Med. 21 (2015) 1280–1289.
[49] J.C. Cohen, E. Boerwinkle, T.H. Mosley Jr., H.H. Hobbs, Sequence variations in PCSK9, low LDL, and protection against coronary heart disease, N. Engl. J. Med. 354 (2006) 1264–1272.
[50] J.J. Repa, D.J. Mangelsdorf, The liver X receptor gene team: potential new players in atherosclerosis, Nat. Med. 8 (2002) 1243–1248.
[51] A.R. Tall, L. Yvan-Charvet, Cholesterol, inflammation and innate immunity, Nat. Rev. Immunol. 15 (2015) 104–116.